

β^+ Decay Partial Half-Life of ^{54}Mn and Cosmic Ray Chronometry

A. H. Wuosmaa, I. Ahmad, S. M. Fischer, J. P. Greene, G. Hackman, V. Nanal, G. Savard, J. P. Schiffer, and P. Wilt

Physics Division, Argonne National Laboratory, Argonne, Illinois 60439

Sam M. Austin and B. A. Brown

National Superconducting Cyclotron Laboratory and Department of Physics and Astronomy, Michigan State University, East Lansing, Michigan 48824

S. J. Freedman

Lawrence Berkeley National Laboratory and Department of Physics, University of California, Berkeley, California 94720

J. J. Connell

Enrico Fermi Institute, University of Chicago, Chicago, Illinois 60637

(Received 25 September 1997)

The weak β^+ decay of the astrophysically significant radioisotope ^{54}Mn has been observed. The energies of positrons from a chemically purified ^{54}Mn source were measured using the APEX spectrometer at Argonne National Laboratory. We deduce a β^+ decay branch of $(1.20 \pm 0.26) \times 10^{-9}$, corresponding to a partial half-life of $(7.1 \pm 1.5) \times 10^8$ yr. The implications of this value for cosmic-ray confinement times are discussed in light of recent satellite measurements of the cosmic-ray abundance of ^{54}Mn . [S0031-9007(98)05458-1]

PACS numbers: 23.40.Hc, 26.40.+r, 27.40.+z, 98.38.-j

The radioisotope ^{54}Mn has attracted considerable interest over the past few years due to its importance as a potential chronometer for galactic cosmic rays (CRs) [1,2]. "Cosmic clocks," such as ^{10}Be or ^{26}Al , are long-lived radioisotopes present in Cosmic Rays, whose abundances, when measured in the solar system, are related to the time they spend traversing the Galaxy. With all its electrons, ^{54}Mn decays essentially 100% of the time via electron capture (EC) to the first excited state of ^{54}Cr at 835 keV. In the high-energy CR environment, however, the nuclei are effectively fully stripped of their electrons, and the EC decay of ^{54}Mn is no longer possible. The lifetime of this isotope is then determined by the much weaker second-forbidden β^- decay to the ground state of ^{54}Fe . This β^- transition is expected to proceed with a partial half-life on the order of ≈ 1 Myr, and makes ^{54}Mn an ideal clock for measuring CR confinement times for elements in the Fe group. Within the context of a given model, the abundance of ^{54}Mn relative to the other Fe group elements is sensitive to both the density of the interstellar medium traversed by the CRs and their galactic confinement times.

Early estimates of the partial half-life of the β^- decay of ^{54}Mn from astronomical measurements yielded a value of $t_{1/2}(\beta^-) \approx 2 \times 10^6$ yr [1]. More recently, direct observation of the isotopic abundance of ^{54}Mn has been achieved [3,4]. Based on these measurements, DuVernois estimated that the β^- partial half-life for ^{54}Mn was between 1 and 2×10^6 yr, assuming a density of the interstellar medium between 0.24 and 0.33 atoms/cm³ [4].

Unfortunately direct experimental determinations of the branch for the weak β^- decay of ^{54}Mn are exceedingly difficult, and have yielded only upper limits which are consid-

erably higher than those suggested by astronomical methods [5]. A measurement of the even weaker β^+ decay to ^{54}Cr is experimentally more feasible due to the additional tag provided by the 511 keV positron annihilation radiation. Sur *et al.* [6] reported an upper limit on the β^+ branch of 4.4×10^{-8} , and da Cruz *et al.* improved this limit to 5.7×10^{-9} [7]. The latter value sets a lower limit on the $^{54}\text{Mn}(\beta^-)$ partial half-life of 2.95×10^5 yr. We present here the results of a measurement of the β^+ decay branch of ^{54}Mn and describe the shell model calculations necessary to obtain from it an estimate of the β^- partial half-life.

The experiment was conducted using the APEX positron spectrometer [8]. The important elements of the spectrometer relevant to the current measurement (see Ref. [8]) are the solenoid which produces the uniform magnetic field which transports positrons to the detector arrays, the silicon arrays used to detect positrons and measure their energies, the NaI arrays which surround the silicon arrays and identify the associated 511 keV annihilation radiation, and the heavy-metal collimators which shield the NaI detectors from the intense flux of photons from the source.

With an end point energy of 355 keV, a large fraction of the positrons from ^{54}Mn β^+ decay have energies less than 150 keV. To improve the response of APEX for low-energy positrons, low threshold (40–50 keV) discriminators were added to the silicon detector electronics. Also, the solenoidal magnetic field was reduced to 200 G to improve the transport efficiency for low-energy positrons.

A number of steps were undertaken so as to ensure that no long-lived positron emitting impurities such as

^{65}Zn ($E_{\text{max}} = 330$ keV, $t_{1/2} = 244.1$ d) and ^{22}Na ($E_{\text{max}} = 546$ keV, $t_{1/2} = 2.6$ yr) were present. The original source material, produced in a reactor by the $^{54}\text{Fe}(n, p)$ reaction, consisted of 2 mCi of $^{54}\text{MnCl}_2$ (material supplied by NEN/Dupont, Boston, MA). A gamma-ray measurement indicated the presence of ^{65}Zn activity in the original sample at the level of $(^{65}\text{Zn}/^{54}\text{Mn}) \approx 5 \times 10^{-5}$. The source material was then passed through two pairs of ion-exchange columns, one pair designed to remove Zn, and the other possible Na impurities. Tests with stable isotopes using identical columns indicated that the suppression factor for each Zn column was $>10^4$, and approximately 300 for each Na column. Each column was counted subsequently to determine the contaminant activity removed from the Mn material. No activity was observed in the second column of each pair, although small amounts of ^{22}Na and ^{65}Zn were observed in the first column of each pair. An independent determination of the lower limits on the suppression factors for these columns obtained by comparing the residual activity in these columns was consistent with the limits obtained using stable element chemistry. The total suppression factors for Zn and Na impurities were $>10^8$ and $\approx 10^5$, respectively. From the measured ^{65}Zn activity present in the original source material and the measured suppression factors, the final concentration of ^{65}Zn in the source was $<5 \times 10^{-13}$. From the residual ^{22}Na observed in the first Na column and the known Na suppression factors, the final concentration of ^{22}Na in the source was $<7 \times 10^{-13}$.

After the separation procedure, the ^{54}Mn was sandwiched between two 1 mg/cm² thick Kapton foils. The mass of the source material was negligible compared to that of the Kapton enclosure. The average activity of the source over the course of the experiment was 756 ± 39 μCi , from counting with an intrinsic Ge detector calibrated to an accuracy of 5% using ^{60}Co and ^{137}Cs sources of known activities. The ^{54}Mn source was counted for a total of 174.9 h live time. The ambient background without source was measured for a period of 57.8 h live time. Subsequently, a ^{65}Zn source prepared on identical Kapton foils was used to determine the efficiency of both the spectrometer and the positron identification procedure. In addition to events from the hardware trigger processor, events from various other sources were prescaled in the master trigger keeping the live time fraction at 75% as measured with a pulser.

The methods used to identify positrons in APEX have been described in Ref. [8]. The most important requirement is the prompt coincidence between a positron detected in the silicon array, and its annihilation photons in two opposing elements of the NaI barrel surrounding that array. The two photon energy signals are required to lie in the 511 keV photopeak, and the reconstructed annihilation position must be within 3.5 cm of a struck element in the silicon array.

A number of sources of background in the measurement can obscure positrons from the source. Cosmic-ray muons can penetrate the NaI barrel as well as the silicon array,

generating a hardware trigger. Some of these events have characteristics of real positrons. While the APEX trigger processor is designed to suppress these events [9], some CRs will evade this suppression. These muons may penetrate the silicon array themselves, producing a true silicon-NaI coincidence, or they may generate a NaI trigger in random coincidence with Compton electrons generated by the 835 keV photons from the source. Scattered photons from the source also induce a random NaI coincidence rate, producing additional random silicon-NaI coincidences. For this experiment the silicon time resolution was degraded to $\approx 1-2$ μs due to the modified discriminators. Cosmic-ray muons typically deposit energy in several NaI detectors, and those penetrating the silicon array strike more than one silicon detector at least 50% of the time. In contrast, $>95\%$ of real positrons with energies less than 400 keV produce signals in only a single silicon wafer and only two NaI bars, as verified by data from the ^{65}Zn source. To suppress CR related backgrounds, events with more than one silicon detector and two NaI bars firing were rejected. These requirements reduced the rate of ambient CR background by a factor of 5, and random coincidences by a factor of 3, relative to an analysis which did not include these gates. The remaining random coincidences were then removed by subtracting data obtained with a random Si-NaI timing gate which was outside the true coincidence window.

The ^{54}Mn positron identification spectrum resulting from this analysis appears in Fig. 1. Here, the data points show the measured Si-NaI position correlation ΔZ for Si-NaI coincidences, after subtraction of random coincidences and ambient background. Real positrons contribute to the peak near $\Delta Z = 0$. Away from this central region, the yield is consistent with 0. For comparison, the histogram is the corresponding spectrum produced by the ^{65}Zn source.

Histograms showing the positron energy spectra for true coincidences (solid line), ambient background (dotted line), random coincidences (thin line), and the sum of randoms and ambient background (dashed line) appear in Fig. 2(a), where all are normalized to the same acquisition live time. The positron energy spectrum corresponding to ^{54}Mn decay is obtained by subtracting random coincidences and ambient background from true coincidences, and is shown in Fig. 2(b). The yield integrated from $E(e^+) = 40$ to 350 keV is 402 ± 79 counts, and from 350 to 1000 keV is -2 ± 45 counts. The solid histogram in Fig. 2(b) represents the spectral shape calculated for the second-forbidden ^{54}Mn β^+ transition, folded with the APEX response. For comparison, the positron energy spectrum from ^{65}Zn , analyzed in the same manner, appears in Fig. 2(c). The histogram in Fig. 2(c) represents the shape calculated for the allowed ^{65}Zn transition folded with the APEX response, and is in reasonable agreement with the data.

The positron detection response of APEX was obtained using a ^{65}Zn source, with small ($\approx 15\%$) corrections from

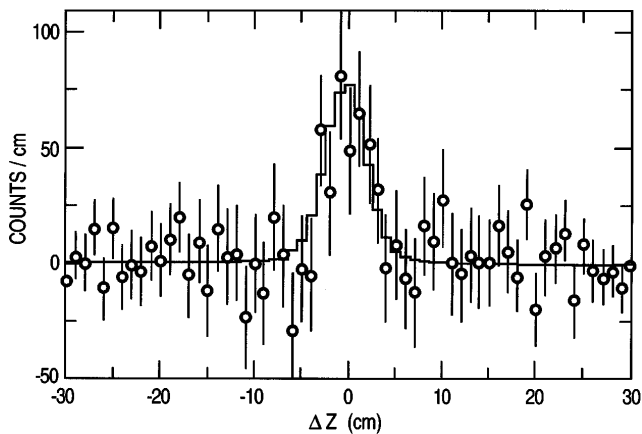


FIG. 1. Positron identification spectra showing the position correlation between hits in the silicon array, and the reconstructed hit position in the NaI barrels. The data points are for ^{54}Mn with background subtracted as described in the text, and the histogram is the spectrum from the ^{65}Zn calibration source, arbitrarily scaled to the ^{54}Mn data.

Monte Carlo simulations which have previously been demonstrated to reproduce the APEX response [8,10]. From the measured yield of positrons from the calibrated ^{65}Zn source, the detection efficiency was experimentally determined (exp) to be $\epsilon(\text{Zn-exp}) = 0.016$ after including all cuts used in the analysis to reduce background. The corresponding Monte Carlo (MC) value was found to be $\epsilon(\text{Zn-MC}) = 0.023$. The same Monte Carlo simulation gives an efficiency for ^{54}Mn positrons of $\epsilon(\text{Mn-MC}) = 0.027$. The difference between the calculated Mn and Zn efficiencies is sensitive only to the different decay spectra. We adopt as our efficiency for positrons from ^{54}Mn $\epsilon(\text{Mn-exp}) = \epsilon(\text{Zn-exp}) \times \frac{\epsilon(\text{Mn-MC})}{\epsilon(\text{Zn-MC})} = 0.019$.

Combined with the average source strength of $756 \pm 39 \mu\text{Ci}$, and the live time of the measurement of 174.9 h, our signal of 402 ± 79 counts then corresponds to a β^+ branching ratio for ^{54}Mn of $(1.20 \pm 0.26) \times 10^{-9}$. The uncertainty is dominated by the counting statistics of the positron measurement, but also contains contributions from the measurement of the strengths of the ^{54}Mn and ^{65}Zn sources. The uncertainty in the efficiency ratio from the Monte Carlo simulations is negligible compared to the statistical error in the data. Combined with the known lifetime for ^{54}Mn EC decay of 312.4 d, our result then corresponds to a β^+ partial decay half-life of $t_{1/2}(\beta^+) = (7.1 \pm 1.5) \times 10^8$ yr.

While we have measured the β^+ partial half-life of ^{54}Mn , the quantity relevant to CR chronology is the faster β^- branch to the ground state of ^{54}Fe . The ratio between these decay rates depends on the available phase space for each transition (the only factor considered previously [6,7]) and their intrinsic β^+ and β^- matrix elements. It is possible that these matrix elements may differ substantially.

We have carried out shell model (SM) calculations using the code OXBASH [11] to obtain estimates of the β^+ and β^- decay strengths of ^{54}Mn . These

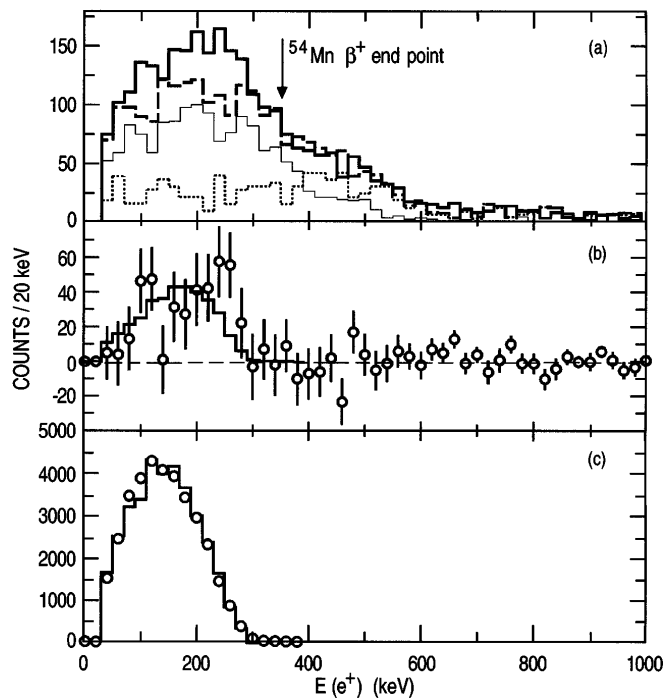


FIG. 2. (a) Histograms of $E(e^+)$, as described in the text. (b) Positron energy spectrum from ^{54}Mn decay, with background subtracted data (points) and the shape expected from the second-forbidden ^{54}Mn decay, folded with the APEX acceptance (histogram). (c) Positron energy spectrum from ^{65}Zn decay (data points) and the calculated allowed shape folded with the APEX acceptance (histogram).

calculations incorporated a truncated SM space of $(0f_{7/2})^{(14-n-r)}(1p_{3/2}0f_{5/2}1p_{1/2})^{n+r}$, where $n = 0, 1,$ and 2 for ^{54}Fe , ^{54}Mn , and ^{54}Cr , respectively, and r , which is either 0 or 1, is the number of additional particles excited outside the $f_{7/2}$ shell [12]. Two different interactions [13,14] were used to estimate the sensitivity of the calculations to the chosen interaction. The results are summarized in Table I. As seen in Table I, rather than being identical, the β^+ and β^- decay matrix elements are calculated to differ by a factor of approximately 2.

In order to estimate the effects of the limited valence space, a calculation involving an analogous unique second-forbidden transition was made in the sd shell using the FPD6 interaction. The ratio between the $B_2(\beta^-)/B_2(\beta^+)$ obtained with the full sd shell and the truncated sd model space, multiplied by the mass 54 value, leads to the table entries labeled “full-shell_{est.}” The observed reduction in the B_2 ratio may, however, represent an overestimate as configuration mixing in the sd shell is stronger than in the fp shell [15].

In the notation of Ref. [16], the calculated second forbidden β^+ decay strength $B_2(\beta^+)$ is related to the partial half-life by $B_2 = C/(f_2 t_{1/2})$, where $C = 6.166 \times 10^{15} \text{ s fm}^4$, $t_{1/2}$ is the partial half-life of the transition, and f_2 is the Fermi integral [17] [$f_2(\beta^-) = 1.496 \times 10^1$, and $f_2(\beta^+) = 2.916 \times 10^{-2}$]. Our measured value of

TABLE I. Shell-model calculation results for ^{54}Mn β^+ and β^- decay.

Valence space	Interaction	$B_2(\beta^+) \rightarrow ^{54}\text{Cr}$	$B_2(\beta^-) \rightarrow ^{54}\text{Fe}$	$\frac{B_2(\beta^-)}{B_2(\beta^+)}$	$B_2(\beta^+) \text{ (exp)}$
$r = 0$ or 1	TBLC8 ^a	9.7 fm ⁴	24.2 fm ⁴	2.5	
$r = 0$ or 1	FPD6 ^b	9.6 fm ⁴	26.4 fm ⁴	2.7	$9.4 \pm 2.0 \text{ fm}^4$
Full shell _{est}	FPD6 ^b	4.8 fm ⁴	8.7 fm ⁴	1.8	

^aInteraction from Ref. [13].

^bInteraction from Ref. [14] with single particle energies adjusted for ^{56}Ni as in [12].

$B_2(\beta^+) = 9.4 \pm 2.0 \text{ fm}^4$ is in excellent agreement with the values calculated with the truncated model space. We expect that the strength ratio $B_2(\beta^-)/B_2(\beta^+)$ should be less sensitive to details of the calculation than absolute quantities, although in the absence of a full fp shell calculation, substantial uncertainty remains. Taking into account the effects of the model-space truncation, and configuration mixing (and assuming that this mixing is half as large as in the sd shell [15]), we estimate a value of $B_2(\beta^-)/B_2(\beta^+) = 2.2 \pm 0.4$ for the mass 54 nuclei. The ± 0.4 represents an estimate of the uncertainty in the theoretical ratio, based upon the fluctuations of the numbers in Table I. The resulting estimate for the β^- partial half-life of ^{54}Mn is then $t_{1/2}(\beta^-) = (6.3 \pm 1.3[\text{stat}] \pm 1.1[\text{theor}]) \times 10^5 \text{ yr}$.

Using this value of the β^- half-life, Fig. 3 shows the dependence of the calculated interstellar density on the fractional abundance of ^{54}Mn , calculated using the ‘‘leaky box’’ model [18] for CR energies of $\approx 310 \text{ MeV/nucleon}$. In this model, CRs, including ionized nuclei such as ^{54}Mn , are trapped in the galaxy for a time τ_{esc} by magnetic fields. There, the CRs interact with material, chiefly neutral hydrogen, in the interstellar medium. Isotopes may be depleted by these interactions, or by radioactive decay as is the case with ^{54}Mn . Our value of $t_{1/2}(\beta^-)$ and the $^{54}\text{Mn}/\text{Mn}$ ratio reported in Ref. [4] yield an inter-

stellar density of $\rho = 0.40(+0.23, -0.15) \text{ atoms/cm}^3$. DuVernois reports that the CR escape time for ^{54}Mn is $\tau_{\text{esc}} \approx 18 \times t_{1/2}(\beta^-)$, or $\tau_{\text{esc}} \approx 11 \text{ Myr}$. These results are in general agreement with those obtained for other CR chronometers, such as ^{10}Be , ^{26}Al , and ^{36}Cl , and imply that CR propagation for Fe-group nuclei is not significantly different from that of lighter isotopes.

The work of the Physics Division, Argonne National Laboratory, is supported by the U.S. Department of Energy, Nuclear Physics Division, under Contract No. W-31-109-Eng-38. The Michigan State University NSCL work is supported by the National Science Foundation, Grants No. PHY95-28844 and No. 96-05207. S.J.F. is supported by U.S. Department of Energy Contract No. DE-AC03-76F0098. J.J.C. is supported in part by ANL-U. of Chicago Grant No. 95-021. We thank R. Firestone for numerical evaluation of the Fermi integrals.

Note added.—After submission of the manuscript, the work of Zaerpoor *et al.* [19] has appeared describing another measurement of ^{54}Mn β^+ decay.

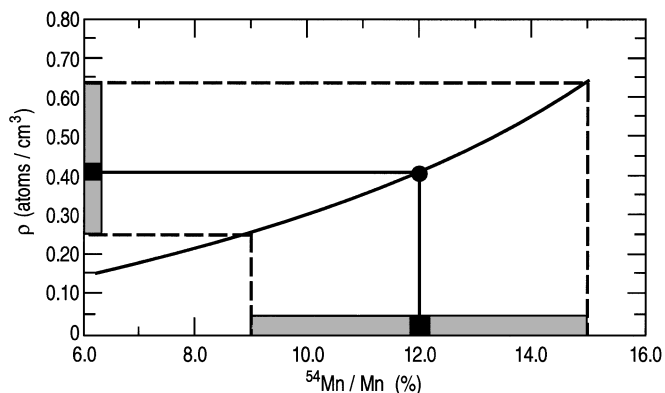


FIG. 3. Deduced interstellar density as a function of the measured ^{54}Mn fractional abundance in cosmic rays, calculated for $t_{1/2}(\beta^-) = 6.3 \times 10^5 \text{ yr}$ and $E(^{54}\text{Mn}) \approx 310 \text{ MeV/nucleon}$. The bar on the abscissa represents the abundance ratio reported by DuVernois, and the bar on the ordinate represents the deduced value of ρ .

- [1] M. Cassé, *Astrophys. J.* **180**, 623 (1973).
- [2] J. E. Grove, B. T. Hayes, and R. A. Mewaldt, *Astrophys. J.* **377**, 680 (1991).
- [3] M. A. DuVernois, *Phys. Rev.* **54**, R2134 (1996).
- [4] M. A. Duvernois, *Astrophys. J.* **481**, 241 (1997).
- [5] T. Kibédi *et al.*, *Astrophys. J.* (to be published).
- [6] B. Sur *et al.*, *Phys. Rev. C* **39**, 1511 (1989).
- [7] M. T. F. da Cruz *et al.*, *Phys. Rev. C* **48**, 3110 (1993).
- [8] I. Ahmad *et al.*, *Nucl. Instrum. Methods Phys. Res., Sect. A* **370**, 539 (1996).
- [9] M. Wolanski *et al.*, *Nucl. Instrum. Methods Phys. Res., Sect. A* **361**, 326 (1995).
- [10] C. M. Conner, Ph.D. thesis, University of Illinois, Chicago, 1997 (unpublished).
- [11] A. Etchegoyen *et al.*, MSU-NSCL Report No. 524, 1985.
- [12] G. Kraus *et al.*, *Phys. Rev. Lett.* **73**, 1773 (1994).
- [13] W. A. Richter *et al.*, *Nucl. Phys.* **A523**, 325 (1991).
- [14] M. G. van der Merwe *et al.*, *Nucl. Phys.* **A579**, 173 (1994).
- [15] J. Rapaport *et al.*, *Nucl. Phys.* **A427**, 332 (1984).
- [16] E. K. Warburton, *Phys. Rev. C* **45**, 463 (1992).
- [17] N. B. Gove and M. J. Martin, *Nucl. Data Tables* **A10**, 205 (1971); R. B. Firestone (private communication).
- [18] J. A. Simpson, *Annu. Rev. Nucl. Part. Sci.* **33**, 323 (1983).
- [19] K. Zaerpoor *et al.*, *Phys. Rev. Lett.* **79**, 4302 (1997).